

Stabilized Finite Element Methods with Anisotropic Mesh Refinement for the Oseen Problem

G. Lube¹, Th. Apel² and T. Knopp³

¹ Math. Fakultät, Georg-August-Universität, D-37083 Göttingen, Germany

`lube@math.uni-goettingen.de`,

² DLR (German Aerospace Center), AS-NV, D-37073 Göttingen, Germany

`Tobias.Knopp@dlr.de`,

³ Inst. für Mathematik und Bauinformatik, Universität der Bundeswehr,

D-85577 München-Neubiberg, Germany

`thomas.apel@unibw.de`

1. Introduction

The starting point of this paper is the nonstationary, incompressible Navier-Stokes problem

$$\partial_t \mathbf{u} - \nu \Delta \mathbf{u} + (\mathbf{u} \cdot \nabla) \mathbf{u} + \nabla p = \mathbf{f} \quad (1)$$

$$\nabla \cdot \mathbf{u} = 0 \quad (2)$$

for velocity \mathbf{u} and pressure p in a domain $\Omega \subset \mathbf{R}^d$, $d \leq 3$. In an outer loop, an A-stable low-order method (possibly with control of the time step Δt) is applied. In an inner loop, we decouple and linearize the resulting system using a Newton-type iteration per time step. This leads to problems of Oseen type:

$$-\nu \Delta \mathbf{u} + (\mathbf{b} \cdot \nabla) \mathbf{u} + c \mathbf{u} + \nabla p = \mathbf{f} \quad \text{in } \Omega \quad (3)$$

$$\nabla \cdot \mathbf{u} = 0 \quad \text{in } \Omega \quad (4)$$

with an artificial reaction term $c \mathbf{u}$ where $c \sim 1/\Delta t$.

We consider stabilized conforming finite element (FE) schemes with equal-order interpolation of velocity/pressure for problem (3)–(4) with emphasis on anisotropic mesh refinement in boundary layers. The classical streamline upwind and pressure stabilization (SUPG/PSPG) techniques for the incompressible Navier-Stokes problem for equal-order interpolation [5], together with additional stabilization of the divergence constraint (4), are well-understood on isotropic meshes [13].

Much less is known about the analysis in case of equal-order interpolation schemes with anisotropic mesh refinement for incompressible flow problems. The Stokes problem has been considered in [3, 4] for the Q1/Q1-case and in [12] for the P1/P1-case. The extension to the Oseen problem seems to be new. Numerical experiments for the full Navier-Stokes problem, e.g. in [9, 7], show the applicability of anisotropic mesh refinement for low-order schemes.

The stabilized FEM for problem (3)–(4) is given in Sec. 2.. In Sec. 3., we derive an a-priori estimate of Cea-type on arbitrary meshes. This result is even valid for rather general finite element pairs for velocity and pressure. In Sec. 4. we focus on hybrid meshes with anisotropic layer refinement of tensor product type and smooth transition to (unstructured) isotropic meshes away from the layer. Sec. 5. is devoted to error estimates and to the design of stabilization parameters. Numerical results for simple channel flows in the laminar and the turbulent case are given in Sec. 6. Full proofs are given in [2].

2. Residual-based stabilized FEM for linearized Navier-Stokes problem

We consider the generalized Oseen model, for brevity with homogeneous Dirichlet data:

$$L_{os}(\mathbf{b}; \mathbf{u}, p) := -\nu \Delta \mathbf{u} + (\mathbf{b} \cdot \nabla) \mathbf{u} + c \mathbf{u} + \nabla p = \mathbf{f} \quad \text{in } \Omega, \quad (5)$$

$$\nabla \cdot \mathbf{u} = 0 \quad \text{in } \Omega, \quad (6)$$

$$\mathbf{u} = \mathbf{0} \quad \text{on } \partial\Omega \quad (7)$$

with $\mathbf{b} \in [H^1(\Omega)]^d$, $(\nabla \cdot \mathbf{b})(x) = 0$, $\mathbf{f} \in [L^2(\Omega)]^d$ and constants $\nu > 0$, $c \geq 0$. The variational formulation reads: find $U := \{\mathbf{u}, p\} \in \mathbf{W} := \mathbf{V} \times \mathbf{Q} := [H_0^1(\Omega)]^d \times L_0^2(\Omega)$ with $L_0^2(\Omega) := \{q \in L^2(\Omega) \mid \int_{\Omega} q \, dx = 0\}$, s.t.

$$\mathcal{A}(\mathbf{b}; U, V) = \mathcal{L}(V) \quad \forall V = \{\mathbf{v}, q\} \in \mathbf{V} \times \mathbf{Q} \quad (8)$$

with

$$\mathcal{A}(\mathbf{b}; U, V) := (\nu \nabla \mathbf{u}, \nabla \mathbf{v})_{\Omega} + ((\mathbf{b} \cdot \nabla) \mathbf{u} + c \mathbf{u}, \mathbf{v})_{\Omega} - (p, \nabla \cdot \mathbf{v})_{\Omega} + (q, \nabla \cdot \mathbf{u})_{\Omega}, \quad (9)$$

$$\mathcal{L}(V) := (\mathbf{f}, \mathbf{v})_{\Omega}. \quad (10)$$

Let \mathcal{T}_h be an admissible triangulation of the polyhedron Ω where each $T \in \mathcal{T}_h$ is a smooth bijective image $T = F_T(\hat{T})$ of a unit element \hat{T} (unit simplex or hypercube in \mathbf{R}^d or, for $d = 3$, the unit triangular prism). A mixture (with appropriate reference elements for each type) is admitted. Consider Lagrangian FE of order $r \in \mathbf{N}$, i. e., $\mathcal{P}_r(\hat{T})$ on \hat{T} contains the polynomial set \mathcal{P}_r . We set

$$X_h^r = \{v \in C(\bar{\Omega}) \mid v|_T \circ F_T \in \mathcal{P}_r(\hat{T}) \, \forall T \in \mathcal{T}_h\} \quad (11)$$

and introduce conforming finite element (FE) spaces for velocity and pressure

$$\mathbf{V}_h^r := [H_0^1(\Omega) \cap X_h^r]^d, \quad \mathbf{Q}_h^s := L_0^2(\Omega) \cap X_h^s, \quad r, s \in \mathbf{N}. \quad (12)$$

The Galerkin method reads: find $U = \{\mathbf{u}, p\} \in \mathbf{W}_h^{r,s} := \mathbf{V}_h^r \times \mathbf{Q}_h^s$, s. t.

$$\mathcal{A}(\mathbf{b}; U, V) = \mathcal{L}(V) \quad \forall V = \{\mathbf{v}, q\} \in \mathbf{W}_h^{r,s}. \quad (13)$$

Well-known sources of instabilities of the Galerkin FEM (13) stem from dominating advection and from the violation of the discrete inf-sup or LBB-condition for $\mathbf{V}_h^r \times \mathbf{Q}_h^s$. Note that, in case of anisotropic elements, the discrete inf-sup constant is often not robust w.r.t. the maximal aspect ratio.

A standard approach to stabilize the Galerkin scheme is a combination of pressure stabilization (PSPG) with streamline-upwind stabilization (SUPG) together with a stabilization of the divergence constraint, the so-called grad-div stabilization. This residual-based stabilized method reads: find $U = \{\mathbf{u}, p\} \in \mathbf{W}_h^{r,s}$, s. t.

$$\mathcal{A}_{rbs}(\mathbf{b}; U, V) = \mathcal{L}_{rbs}(V) \quad \forall V = \{\mathbf{v}, q\} \in \mathbf{W}_h^{r,s} \quad (14)$$

with

$$\begin{aligned} \mathcal{A}_{rbs}(\mathbf{b}; U, V) &:= \mathcal{A}(\mathbf{b}; U, V) + \sum_{T \in \mathcal{T}_h} \gamma_T (\nabla \cdot \mathbf{u}, \nabla \cdot \mathbf{v})_T \\ &\quad + \sum_{T \in \mathcal{T}_h} (L_{os}(\mathbf{b}; \mathbf{u}, p), \delta_T((\mathbf{b} \cdot \nabla) \mathbf{v} + \nabla q))_T \end{aligned} \quad (15)$$

$$\mathcal{L}_{rbs}(V) := \mathcal{L}(V) + \sum_{T \in \mathcal{T}_h} (\mathbf{f}, \delta_T((\mathbf{b} \cdot \nabla) \mathbf{v} + \nabla q))_T. \quad (16)$$

Remark 1. A crucial point in the numerical analysis is the Galerkin orthogonality

$$\mathcal{A}_{rbs}(\mathbf{b}; U - U_h, V_h) = 0 \quad \forall V_h \in \mathbf{W}_h^{r,s}. \quad (17)$$

Other residual-based variants, containing the SUPG-/PSPG-stabilization with $\delta_T = \delta_T^u = \delta_T^p$, are the Galerkin/ Least-squares (GLS) method [8] and the Douglas/Wang- or algebraic subgrid-scale (ASGS) method [6] adding

$$\sum_{T \in \mathcal{T}_h} (L_{Os}(\mathbf{b}; U) - \mathbf{f}, \delta_T L_{Os}(\mathbf{b}; V))_T$$

and

$$- \sum_{T \in \mathcal{T}_h} (L_{Os}(\mathbf{b}; U) - \mathbf{f}, \delta_T L_{Os}^*(\mathbf{b}; V))_T,$$

respectively, to the Galerkin formulation (13). The analysis of these methods is similar to that of scheme (14)-(16). \square

3. Stability and convergence on arbitrary meshes

The subsequent analysis provides existence, uniqueness and a generalized result of Cea type for the discrete solution without geometrical conditions on the mesh. Stability of the residual-based method (14)-(16) with $\delta_T = \delta_T^u = \delta_T^p$ is proved w.r.t.

$$\|V\|_{rbs}^2 := \|\nu^{\frac{1}{2}} \nabla \mathbf{v}\|_{L^2(\Omega)}^2 + \|c^{\frac{1}{2}} \mathbf{v}\|_{L^2(\Omega)}^2 + J_{rbs}(V, V), \quad (18)$$

$$J_{rbs}(V, V) := \sum_T \delta_T \|(\mathbf{b} \cdot \nabla) \mathbf{v} + \nabla q\|_{L^2(T)}^2 + \sum_T \gamma_T \|\nabla \cdot \mathbf{v}\|_{L^2(T)}^2 \quad (19)$$

with parameters δ_T, γ_T to be determined. A simplified analysis is possible since $\|\cdot\|_{rbs}$ is a mesh-dependent norm on $\mathbf{W}_h^{r,s}$ if $\delta_T > 0$.

Consider a (possibly anisotropic) element $T \subset \mathbb{R}^d$, $d = 2, 3$, with sizes $h_{1,T} \geq \dots \geq h_{d,T}$. A key point in the stability analysis is the local inverse inequality

$$\|\Delta \mathbf{w}\|_{[L^2(T)]^d} \leq \mu_{inv} h_{d,T}^{-1} \|\nabla \mathbf{w}\|_{[L^2(T)]^{d \times d}} \quad \forall \mathbf{w} \in \mathbf{V}_h^r. \quad (20)$$

to bound the term $\Delta \mathbf{u}_h$ in the SUPG-term in (15). Assume that the conditions

$$0 < \delta_T \leq \frac{1}{2} \min \left\{ \frac{h_{d,T}^2}{\mu_{inv}^2 \nu}; \frac{1}{c} \right\}, \quad 0 \leq \gamma_T. \quad (21)$$

on the stabilization parameters are satisfied. In view of (21), the upper bound of the stabilization parameter δ_T is related to $h_{d,T}$. The inverse inequality (20) and (21) imply that the bilinear form $\mathcal{A}_{rbs}(\mathbf{b}; \cdot, \cdot)$, defined in (15), satisfies

$$\mathcal{A}_{rbs}(\mathbf{b}; W_h, W_h) \geq \frac{1}{2} \|W_h\|_{rbs}^2, \quad \forall W_h \in \mathbf{W}_h^{r,s}. \quad (22)$$

This implies existence and uniqueness of the discrete solution of (14)-(16).

The following continuity result is derived using standard inequalities. It reflects the effect of stabilization with assumption (21): For each $U \in \mathbf{W}$ with $\Delta \mathbf{u}|_T \in [L^2(T)]^d \forall T \in \mathcal{T}_h$ and $V_h \in \mathbf{W}_h^{r,s}$ there holds

$$\mathcal{A}_{rbs}(\mathbf{b}; U, V_h) \leq \mathcal{Q}_{rbs}(U) \|V_h\|_{rbs} \quad (23)$$

with

$$\begin{aligned} \mathcal{Q}_{rbs}(U) &:= \llbracket U \rrbracket_{rbs} + \left(\sum_{T \in \mathcal{T}_h} \frac{1}{\delta_T} \|\mathbf{u}\|_{L^2(T)}^2 \right)^{\frac{1}{2}} + \left(\sum_{T \in \mathcal{T}_h} \frac{1}{\max(\nu, \gamma_T)} \|p\|_{L^2(T)}^2 \right)^{\frac{1}{2}} \\ &\quad + \left(\sum_{T \in \mathcal{T}_h} \delta_T \|\nu \Delta \mathbf{u} + c\mathbf{u}\|_{L^2(T)}^2 \right)^{\frac{1}{2}}. \end{aligned} \quad (24)$$

The L^2 -terms in (24) explode for $\nu, c \rightarrow 0$ and vanishing stabilization with $\delta_T = \gamma_T = 0$.

The standard combination of the stability and continuity estimates (22) and (23) with Galerkin orthogonality (17) leads to the desired error estimate of Cea-type. Consider solutions $U \in \mathbf{W}$ and $U_h \in \mathbf{W}_h^{r,s}$ of the continuous and of the discrete problem, respectively. Let $\{I_{h,r}^u \mathbf{u}, I_{h,s}^p p\} \in \mathbf{W}_h^{r,s}$ be an appropriate interpolant of U , e.g., the Lagrange interpolant. Then we obtain an quasi-optimal a-priori estimate of Cea-type for the scheme (14)-(16):

$$\llbracket U - U_h \rrbracket_{rbs} \leq \mathcal{Q}_{rbs}(\{\mathbf{u} - I_{h,r}^u \mathbf{u}, p - I_{h,s}^p p\}). \quad (25)$$

It remains to evaluate the right hand side of (25) using appropriate interpolation estimates and to fix the parameter sets $\{\delta_T\}$ and $\{\gamma_T\}$.

4. Stability and convergence on hybrid meshes

The quasi-optimal a-priori result (25) provides no control of the L^2 -norm of the pressure. Therefore we analyze the stabilized method (14)-(16) w.r.t. the norm

$$\|V\|_{rbs} := \left(\llbracket V \rrbracket_{rbs}^2 + \sigma \|q\|_{L^2(\Omega)}^2 \right)^{\frac{1}{2}} \quad (26)$$

with parameter σ to be determined. Here we present a discrete inf-sup condition and a quasi-optimal error estimate w.r.t. $\|\cdot\|$. For simplicity, we restrict ourselves to the case of *equal-order* interpolation of velocity/pressure, i.e., to $r = s$.

Of practical interest are *hybrid* meshes with *anisotropic* mesh refinement of tensor product type (in the sense of [1, Chap. 3]) in the boundary layer and a smooth transition to (in general unstructured) shape-regular (isotropic) meshes away from the layer. We restrict ourselves to the case that the boundary layer is located at the hyperplane $x_d = 0$. The advantage of this class of meshes is not only that the coordinate transformation is simplified in regions with anisotropic elements but also that certain edges/faces of the elements are orthogonal/parallel to coordinate axes. This is exploited in the analysis. Fig. 1 shows examples of such meshes for the two- and three-dimensional case.

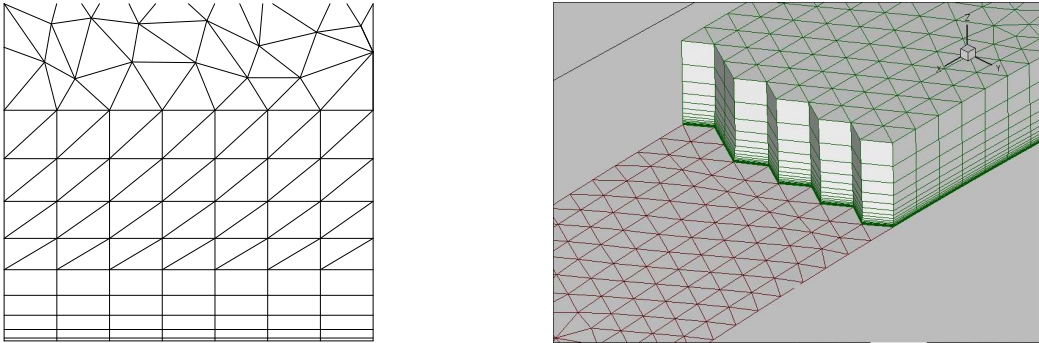


Figure 1: Examples of hybrid meshes in the two- and three-dimensional case

Meshes of tensor product type in the boundary layer region consist of affine elements of tensor product type. That means the transformation of a reference element \hat{T} to the element T

shall have (block) diagonal form,

$$x = \begin{pmatrix} A_T \vdots 0 \\ \dots\dots\dots \\ 0 \vdots \pm h_{d,T} \end{pmatrix} \hat{x} + \mathbf{a}_T \quad \text{for ,} \quad (27)$$

where $\mathbf{a}_T \in \mathbb{R}^d$, $A_T = \pm h_{1,T}$ for $d = 2$ and $A_T \in \mathbb{R}^{2 \times 2}$ for $d = 3$ with $|\det A_T| \sim h_{1,T}^2$, $\|A_T\| \sim h_{1,T}$, $\|A_T^{-1}\| \sim h_{1,T}^{-1}$. In this way the element sizes $h_{1,T}, \dots, h_{d,T}$ are implicitly defined. Note that the additional conditions yield $h_{1,T} \sim h_{2,T}$ for $d = 3$.

Under these assumptions, the triangles/tetrahedra can be grouped into pairs/triples which form a rectangle/triangular prism of tensor product type. We demand further that there is no abrupt change in the element sizes, that means $h_{i,T} \sim h_{i,T'}$ for all T' with $\overline{T} \cap \overline{T'} \neq \emptyset$, $i = 1, \dots, d$. This implies that the transition region between the structured mesh in the boundary layer zone and the unstructured mesh consists of isotropic elements only. In particular, Shishkin's piecewise equidistant meshes in boundary layers are excluded.

Here, we consider *equal-order* interpolation, i.e., $r = s \geq 1$. Condition (21) has to be refined as

$$0 < \mu_0 h_{1,T}^2 \leq \delta_T \leq \frac{1}{2} \min \left\{ \frac{h_{d,T}^2}{\mu_{inv}^2 \nu}; \frac{1}{c} \right\}, \quad 0 \leq \delta_T \|\mathbf{b}\|_{[L^\infty(T)]^d}^2 \leq \gamma_T. \quad (28)$$

with some constant $\mu_0 > 0$ (see Remark 2). Then there exists a positive constant β , independent of all important parameters ($\nu, c, h_{1,T}, \dots, h_{d,T}$, aspect ratio, δ_T, γ_T) such that the modified inf-sup condition

$$\inf_{U_h \in \mathbf{W}_h^{r,s}} \sup_{V_h \in \mathbf{W}_h^{r,s}} \frac{\mathcal{A}_{rbs}(\mathbf{b}; U_h, V_h)}{\|U_h\|_{rbs} \|V_h\|_{rbs}} \geq \beta \quad (29)$$

with the weight

$$\sqrt{\sigma} \sim \left(\sqrt{\gamma} + \frac{1}{\mu_0} + \sqrt{\nu} + \sqrt{c} C_F + \frac{C_F \|\mathbf{b}\|_{L^\infty(\Omega)}}{\sqrt{\nu + c C_F^2}} + \max_T \frac{h_T \|\mathbf{b}\|_{L^\infty(T)}}{\sqrt{\nu}} \right)^{-1} \quad (30)$$

of the L^2 -norm of the pressure in (26). Moreover, it denotes $\gamma = \max_{T \in \mathcal{T}_h} \gamma_T$ and C_F the Friedrichs constant. Note that σ is only used for the analysis. A critical point in the stability analysis is the following interpolation result for a modified Scott-Zhang quasi-interpolation operator $I_{h,r}^{qi} : H^1(\Omega) \rightarrow X_h^r$:

$$\|\nabla^m (v - I_{h,r}^{qi} v)\|_{L^2(T)} \leq C_{qi,m} h_{1,T}^{1-m} \|v\|_{H^1(\omega_T)}, \quad m = 0, 1 \quad (31)$$

where $\omega_T := \bigcup_{\overline{T'} \cap \overline{T} \neq \emptyset} T'$. (31) can be derived using ideas of [1, Chap. 3.4].

A combination of (29) with the continuity estimate (24) leads again to a modified quasi-optimal estimate (25) of Cea type where we replace the $\|[\cdot]\|_{rbs}$ -norm by the $\|\cdot\|_{rbs}$ -norm.

Remark 2. The lower bound of δ_T in assumption (28) implicitly implies

$$\sqrt{\mu_0} \max_{T \in \mathcal{T}_h} \frac{h_{1,T}}{h_{d,T}} \leq \frac{1}{\mu_{inv} \sqrt{2\nu}} \quad (32)$$

with a restriction on the aspect ratio of T . A reasonable choice in boundary layers at a wall is $h_{d,T} \geq \sqrt{\nu} h_{1,T}$; thus guaranteeing that $\mu_0 = \mathcal{O}(1)$, see also Sect. 5.. \square

5. Error estimates and design of stabilization parameters

Based on the quasi-optimal of Section 4., we derive error estimates and design the parameters δ_T, γ_T with emphasis on the anisotropy of an element. Here, we assume that the solution of problem (5)-(7) is smooth enough such that the global Lagrangian interpolant can be used.

Appropriate anisotropic interpolation estimates of the FE spaces X_h^r are required in order to compensate large derivatives in some direction x_d by the small element diameter $h_{d,T}$. We refer to [1] for a basic interpolation theory which relies on some geometrical conditions (maximal angle condition and the coordinate system condition) which are valid for the hybrid meshes introduced in Sec. 4.. The anisotropic interpolation result for the Lagrangian interpolation operator $I_{h,r} : \mathbf{C}(\bar{T}) \rightarrow \mathcal{P}_r(T)$ reads as follows, see [1, Chap. 3].

Let \mathcal{T}_h be a hybrid mesh as introduced in Section 4., and $T \in \mathcal{T}_h$. Assume that $v \in W^{\ell,p}(T)$, with $\ell \in \{1, \dots, r+1\}$, $p \in [1, \infty]$, such that $p > 2/\ell$. Fix $m \in \{0, \dots, \ell-1\}$. Then the following estimate holds

$$\|v - I_{h,r}v\|_{W^{m,p}(T)} \leq C \sum_{|\alpha|=\ell-m} \mathbf{h}_T^\alpha \|D^\alpha v\|_{W^{m,p}(T)} \quad \mathbf{h}_T^\alpha := h_1^{\alpha_1} \dots h_d^{\alpha_d}. \quad (33)$$

Assume that the solution $U = \{\mathbf{u}, p\} \in \mathbf{W}$ is continuous and satisfies $\mathbf{u}|_T \in [H^k(T)]^d$, $p|_T \in H^k(T)$ with $k > 1$ for all $T \in \mathcal{T}_h$. Then, using the notation $l := \min(r, k-1)$ for the convergence order, we obtain

$$\|U_h\|_{rbs}^2 \leq \sum_T \sum_{|\alpha|=l, |\beta|=1} \mathbf{h}_T^{2\alpha} \left(E_{T,\beta}^p \|D^{\alpha+\beta} p\|_{L^2(T)}^2 + E_{T,\beta}^u \|D^{\alpha+\beta} \mathbf{u}\|_{L^2(T)}^2 \right), \quad (34)$$

$$E_{T,\beta}^p := \delta_T + \gamma_T^{-1} \mathbf{h}_T^{2\beta} \quad (35)$$

$$E_{T,\beta}^u := \nu + ch_{1,T}^2 + \gamma_T + \delta_T \|\mathbf{b}\|_{[L^\infty(T)]^d}^2 + \delta_T^{-1} \mathbf{h}_T^{2\beta}. \quad (36)$$

The mixed character of the problem requires a careful approach to fix the parameters δ_T, γ_T . Using $\tilde{h}_T \in [h_{d,T}, h_{1,T}]$ and based on assumption (28), we propose to define the parameters according to

$$\delta_T \sim \min \left(\frac{h_{d,T}^2}{\mu_{inv}^2 \nu}; \frac{1}{c}; \frac{\tilde{h}_T}{\|\mathbf{b}\|_{(L^\infty(T))^d}} \right), \quad \gamma_T \sim \frac{\tilde{h}_T^2}{\delta_T}. \quad (37)$$

In the isotropic region Ω_{iso} away from the boundary layer, we propose to set $h_{1,T} \sim \tilde{h}_T$ which leads to the standard design and to the standard error contributions (see [8, 6]).

The parameter design in the boundary layer region Ω_{aniso} at $x_d = 0$ is more involved. The crucial point is that the (anisotropic) mesh allows a resolution of the scale $\sqrt{\nu}$ at the wall. From Prandtl's boundary layer theory for laminar flows, we know that p varies at most slowly with x_d , whereas \mathbf{u} can have large gradients in x_d -direction. This motivates a mesh refinement in x_d -direction towards the wall by setting $h_{d,T} \sim g(x_d)h_{1,T}$ with a strongly increasing monitor function $g(\cdot)$ s.t. $g(x_d) \sim \sqrt{\nu}$ in the mesh layer nearest to the wall and $g(x_d) \sim 1$ in the transition region to the isotropic part of the hybrid mesh.

The velocity error part in the error contribution (30) contains the critical term $\delta_T^{-1} h_T^{2\beta}$ which is at most of order $\mathcal{O}(1)$ in the mesh layer nearest to the wall at $x_d = 0$ since $h_{d,T} \sim \sqrt{\nu} h_{1,T}$. On the other hand, we observe that the stabilization parameters do not deteriorate there since $\nu^{-1} h_{d,T}^2 \sim h_{1,T}^2$.

It remains to discuss the choice of \tilde{h}_T . We obtain from (37) that an increasing \tilde{h}_T implies an increasing γ_T , thus giving improved control of $\nabla \cdot \mathbf{u}$. On the other hand, the control parameter $\sqrt{\sigma}$ of $\|p - p_h\|_{L^2(\Omega)}$ behaves like $1/\sqrt{\sigma} \leq \max_T \sqrt{\gamma_T}$, i.e. the control of this norm gets worse with increasing γ_T . Our favoured choice is $\tilde{h}_T = (\text{meas}(T))^{1/d}$, as a reasonable compromise to balance control of pressure and of divergence.

6. Application to channel flow

We present some numerical results for the Navier-Stokes problem (1)-(2) using the research code *Parallel NS* with P1-approximations for velocity/pressure.

Consider the *laminar* stationary flow in the channel $\Omega = (0, 1)^2$ with the data $\nu = 10^{-6}$, $\mathbf{b} = \mathbf{u}$, $c = 0$, $\mathbf{f} = \mathbf{0}$ and solution $p = \sqrt{\nu}(1 - x)$, $\mathbf{u} = (1 - (e^{-y/\sqrt{\nu}} + e^{(y-1)/\sqrt{\nu}}), 0)^T$. The layer-adapted hybrid mesh is equidistant in x -direction and has a mesh grading in y -direction with $y_i = \frac{1}{2} + \frac{1}{2} \tanh(\frac{2i\gamma}{N_y-1}) / \tanh(\gamma)$, $i = -\frac{1}{2}(N_y - 1), \dots, \frac{1}{2}(N_y - 1)$. The parameter γ can be chosen such that condition (30) holds with $\mu_0 = \mathcal{O}(1)$.

In Fig. 2 (left), we show the pointwise error $(u_1 - u_{1,h})(\frac{1}{2}, y)$, $0 \leq y \leq 1$ for increasing values of N_y . In Fig. 2 (right), we present a zoom in a semilogarithmic scale for fixed $N_y = 129$ together with different values of γ (leading to different percentage of mesh points in the boundary layer regions $(0, 1) \times (0, \delta_{99})$ and $(0, 1) \times (1 - \delta_{99}, 1)$ where δ_{99} is given by $u_1(x, \delta_{99}) = (0.99, 0)$). On the grid with $N_y = 129$, the L^∞ -error is reduced to $\leq 0.2\%$ if 37.5 or 50 % of the grid points are located in the layer regions for resolving the gradient, whereas the solution on the corresponding uniform mesh has a L^∞ -error of 10 %.



Figure 2: Error $(u_1 - u_{1,h})(\frac{1}{2}, y)$ (left) and zoom for $N_y = 129$ (right)

Finally, we consider the *turbulent* 3d-channel flow in $\Omega = (0, H)^2 \times (0, L)$ with $H = 1$ [m] and $L = 5$ [m]. We apply the $k - \epsilon - \bar{v}^2 - \bar{f}$ -model of Durbin in the "user-friendly" $\varphi - \bar{f}$ -version [11] for the RANS version of problem (1)-(2) where the viscosity ν is replaced with $\nu_e = \nu + \nu_t$ based on the turbulent viscosity $\nu_t = c_\mu k \varphi \max(\frac{k}{\epsilon}, 6\sqrt{\frac{\nu}{\epsilon}})$. The turbulent quantities $k, \epsilon, \varphi, \bar{f}$ are determined by a coupled nonlinear advection-diffusion-reaction system.

We compare the solution to DNS data of [10] for $Re_\tau = \frac{H u_\tau}{\nu} = 395$ based on the friction velocity $u_\tau = \sqrt{\tau_w} \equiv \sqrt{\nu \frac{\partial u_2}{\partial y}|_{\Gamma_w}} = 1.2087 \cdot 10^{-2}$. This corresponds to $Re_C = \frac{U_C H / 2}{\nu} \approx 14.000$. Moreover, we have $\mathbf{f} = \frac{\tau_w}{H} \mathbf{e}_x$. Our calculations are performed on a FE-mesh with $33 \times 49 \times 65$ nodes. In y -direction, we use the above tanh-distribution with γ s.t. the first off-wall node is at $y u_\tau / \nu = 1$. The sets δ_T, γ_T are based on $\tilde{h}_T = |\text{meas}(T)|^{\frac{1}{3}}$.

In Fig. 3, we present the relevant quantities $u^+ = \frac{u_1}{u_\tau}$ and $k^+ = \frac{k}{u_\tau^2}$ in wall units at $x = 3$ [m] and $x = 4.5$ [m] in wall units. The results are in reasonable agreement with the DNS data and even better than results presented in [11].

Acknowledgment: We thank M. Wannert and R. Gritzki for performing the numerical results for the laminar and turbulent test problems.

References

- [1] Apel, Th.: *Anisotropic finite elements: Local estimates and applications*. Series "Advances in Numerical Mathematics", Teubner, Stuttgart, 1999.

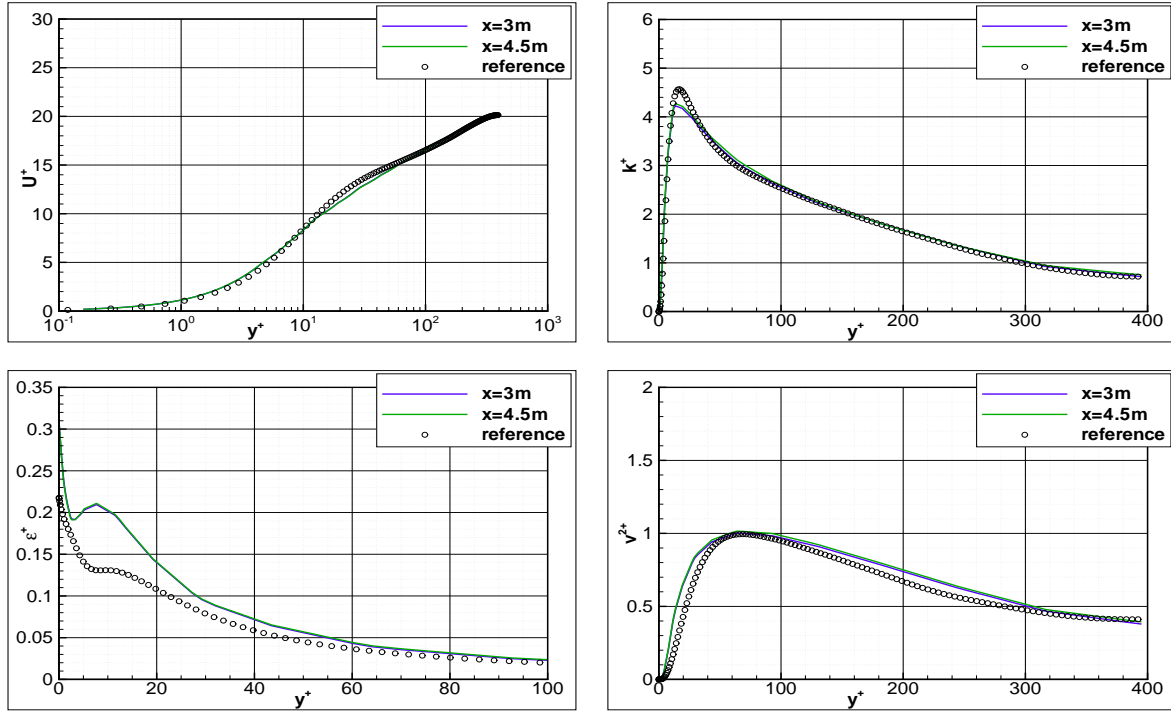


Figure 3: Plot of $u^+, k^+, \epsilon^+, (v^2)^+$ vs. $y^+ := \frac{yu_\tau}{\nu}$ at $x \in \{3, 4.5\}$ [m]

- [2] Apel, T., Knopp, T., Lube, G.: *Stabilized finite element methods with anisotropic mesh refinement for the Oseen problem*, submitted to APNUM.
- [3] Becker, R., Rannacher, R.: *Finite element solution of the incompressible Navier-Stokes equations on anisotropically refined meshes*, Notes Numer. Fluid Mech., 49 (1995), 52–62.
- [4] Braack, M., Richter, Th.: *Local projection stabilization for the Stokes system on anisotropic quadrilateral meshes.*, to appear in: Proceed. ENUMATH 2005, Springer, pp. 791–798.
- [5] Brooks, A.N., Hughes, T.J.R.: *Streamline upwind Petrov-Galerkin formulation for convection dominated flows with particular emphasis on the incompressible Navier-Stokes equations*, CMAME 32 (1982), 199–259.
- [6] Codina, R.: *Stabilization of incompressibility and convection through orthogonal subscales in finite element methods*, CMAME 190 (13/14) (2000) 1579–1599.
- [7] Codina, R., Soto, O.: *Approximation of the incompressible Navier-Stokes equations using orthogonal subscale stabilization and pressure segregation on anisotropic finite element meshes*, CMAME 193 (2004) 1403–1419.
- [8] Franca, L.P., Frey, S.L.: *Stabilized finite element methods. II. The incompressible Navier-Stokes equations*, CMAME 99 (1992) 209–233.
- [9] Hughes, T.J.R., Jansen, K.: *A stabilized finite element formulation for the Reynolds-averaged Navier-Stokes equations*, Surv. Math. Ind. (1995) 4: 279–317.
- [10] Kim, J., Moin, P., Moser, R.: *Turbulence statistics in fully developed channel flow at low Reynolds number*, J. Fluid Mech. 177 (1987) 133–166.
- [11] Laurence, L.R., Uribe, J.C., Utyuzhnikov, S.V.: *A robust formulation of the v_2-f model*, J. Flow, Turbulence and Combustion 23 (2004) 169–185.
- [12] Micheletti, S., Perotto, S., Picasso, M.: *Stabilized finite elements on anisotropic meshes: A priori error estimates for the advection-diffusion and the Stokes problems*. SINUM 41 (2003) 3, 1131–1162.
- [13] Tobiska, L., Verfürth, R.: *Analysis of a streamline-diffusion finite element method for the Stokes and Navier-Stokes equations*, SINUM 33 (1996), 107–127.